

Alloy formation in the system Au(1 1 1)/Cd during the UPD process

M.C. del Barrio, S.G. García, D.R. Salinas *

*Instituto de Ing. Electroquímica y Corrosión (INIEC), Departamento de Ingeniería Química, Universidad Nacional del Sur,
Avda. Alem 1253, 8000 Bahía Blanca, Argentina*

Received 4 May 2004; received in revised form 25 May 2004; accepted 25 May 2004
Available online 17 June 2004

Abstract

The Au–Cd alloy formation in the course of Cd underpotential deposition (UPD) in the system Au(1 1 1)/Cd²⁺, SO₄²⁻ has been studied by conventional electrochemical techniques and in situ STM. The long time polarization experiments and the current–potential desorption spectra have indicated that the alloy can be formed at relatively high underpotentials with the formation of 2D Cd islands as was observed by in situ STM images. These islands grow and coalesce at a constant potential with the subsequent formation of new 2D islands on top of the partially formed first Cd monolayer. Atomically resolved images of these islands have revealed an hexagonal atomic structure with an interatomic distance of 0.29 ± 0.01 nm. The dissolution of these features occurs together with the formation of many holes of monatomic height which induces a surface roughening. The alloy formation is explained considering a place exchange process between the Au atoms and the adsorbed Cd atoms followed by solid state diffusion of these atoms through the alloyed phase.

© 2004 Elsevier B.V. All rights reserved.

Keywords: Alloy formation; Cd UPD; Au(1 1 1); In situ STM

1. Introduction

The underpotential deposition (UPD) process of different metals on well-characterized single crystal surfaces such as Au(*hkl*), has been widely studied [1,2]. Initially, the main interest was focussed on the structural properties of both the single crystal surfaces and the low dimensional metal phases formed. In the last years there has been increasing attention in studying the structure, growth and properties of surface alloy films formed during the Me UPD. In this sense, Cd is known to produce intermetallic phases on Au in the UPD region during long time polarization experiments [3]. The Cd UPD on gold substrates appears as an interesting process due to its promising application for high quality thin film semiconductor devices [4] and its catalytic properties for the electroreduction of nitrate anions [5,6]. Gewirth and coworkers [7,8] have studied the system Au(1 1 1)/Cd²⁺, SO₄²⁻ in the UPD range using

STM and quartz crystal microbalance. They have observed different ordered lattices and concluded that sulphate is specifically adsorbed with underpotentially deposited Cd. Nevertheless, no information was indicated about surface alloy formation during the course of these experiments. Inzelt and Horányi [9] have studied the Cd UPD on polycrystalline gold using the electrochemical microbalance technique and they concluded that the Au–Cd alloy is formed during the UPD phenomenon probably by a turnover process between the adsorbed Cd and the underlying Au atoms, with a subsequent solid-state diffusion of these atoms through the alloyed phase. This suggestion was based on the model proposed by Vidu and Hara [10–13] for the alloy formation process observed in the system Au(1 0 0)/Cd²⁺, SO₄²⁻. Mizuki and coworkers [14] using specular X-ray reflectivity measurements, have also indicated that the Cd UPD layer formed on Au(1 1 1) in sulphuric acid solution consists of both a Cd atomic layer and a sulphate anion layer. However, the alloy formation process was not clear from their results. Stickney and coworkers [15,16], Lee and Rayment [17] and Schmucki

* Corresponding author. Fax: +54-291-4595182.

E-mail address: dsalinas@criba.edu.ar (D.R. Salinas).

and coworkers [18–20] have indicated that the Cd UPD is also possible on the reconstructed surface of Au(111) without lifting the reconstruction. These authors have also observed that Cd UPD results in the alloying of adsorbed Cd atoms with Au atoms from the surface.

All the studies referenced above were performed in the underpotential range where Cd UPD peaks are clearly observed. The aim of the present paper is to get further insight into the Cd UPD process in the system Au(111)/Cd²⁺, SO₄²⁻. The work is focussed on the formation of the Au–Cd alloy at relatively high underpotentials, using conventional electrochemical techniques and in situ STM analysis.

2. Experimental

The experiments were performed in the systems Au(111)/SO₄²⁻ and Au(111)/Cd²⁺, SO₄²⁻ using a Au(111) single crystal electrode with a diameter of 0.4 cm. The substrate surface was first mechanically polished with diamond paste of decreasing grain size down to 0.25 μm and subsequently electrochemically polished in a cyanide bath according to a standard procedure [21]. The pre-treatment procedure prior to each measurement was already previously described [22].

The electrolyte solutions used throughout the study were 5 mM H₂SO₄ + 0.1 M Na₂SO₄ and 5 mM H₂SO₄ + 0.1 M Na₂SO₄ + 1 mM CdSO₄. These solutions were prepared from suprapure chemicals (Merck, Darmstadt) and fourfold quartz-distilled water, and deaerated by nitrogen bubbling prior to each experiment.

Conventional electrochemical studies were performed in a standard three-electrode electrochemical cell. The counter electrode was a platinum sheet (1 cm²) and the reference electrode was a Hg/Hg₂SO₄/K₂SO₄ saturated electrode (SSE), mounted inside a Luggin capillary. The actual electrode potential, E , is referred to the SSE, whereas the underpotential, ΔE , is related to the Nernst equilibrium potential of the 3D Cd phase by $\Delta E = E - E_{3D Cd}$, with $E_{3D Cd} = -1150$ mV for $c_{Cd^{2+}} = 1$ mM. The measurements were carried out with a potentiostat–galvanostat EG&G Princeton Applied Research Model 273A.

An standard Nanoscope III equipment (Digital Instruments, Santa Barbara, CA, USA) was used for the in situ STM studies, employing Apiezon insulated Pt–Ir tips (Digital Instruments, Santa Barbara, USA). Pt wires were used as counter- and quasi-reference electrode. The potentials of the gold substrate and the STM tip were controlled independently by a Nanoscope III-bipotentiostat optimised for the STM set-up used. The tip potential was held constant at a value of minimum faradaic current and the tip current varied in the range $2 \leq I_{tun}/nA \leq 20$. The experimental set-up for the in situ

STM technique has been checked by cyclic voltammetric measurements and the results were identical to those obtained in the conventional electrochemical cell.

3. Results and discussion

3.1. Electrochemical experiments

Fig. 1 shows typical cyclic voltammograms obtained for the systems Au(111)/SO₄²⁻ and Au(111)/Cd²⁺, SO₄²⁻. For the Cd²⁺ free solution the typical and very extensive double layer region of the substrate is observed, together with broad current peaks in the potential range $-300 \leq E_{SSE}/mV \leq 400$ that are ascribed to anion adsorption [23,24]. For the solution containing Cd²⁺ ions, the Cd UPD on Au(111) is clearly observed at $0 \leq \Delta E/mV \leq 750$. In agreement with other authors [7,18], two different adsorption/desorption current peaks were recorded at $\Delta E_{A_2/D_2} \approx 650$ mV and $\Delta E_{A_3/D_3} \approx 330$ mV. Another adsorption/desorption peak, A₄/D₄, not shown in Fig. 1, is also present at underpotentials close to the equilibrium potential [18]. By comparing the cyclic voltammograms obtained in both solutions, in the presence of Cd²⁺ ions it is also possible to note a slight increase in the circulated charge in the potential range $750 \leq \Delta E/mV \leq 1350$ (A₁ region). Furthermore, at $\Delta E = 1580$ mV appears an anodic UPD peak (D₁) which overlaps with one of those related to the anion adsorption. The presence of peak D₁ was not previously reported by other authors. Additionally, a remarkable observation is that a repetitive cycling experience performed in the potential range $150 \leq \Delta E/mV \leq 1350$

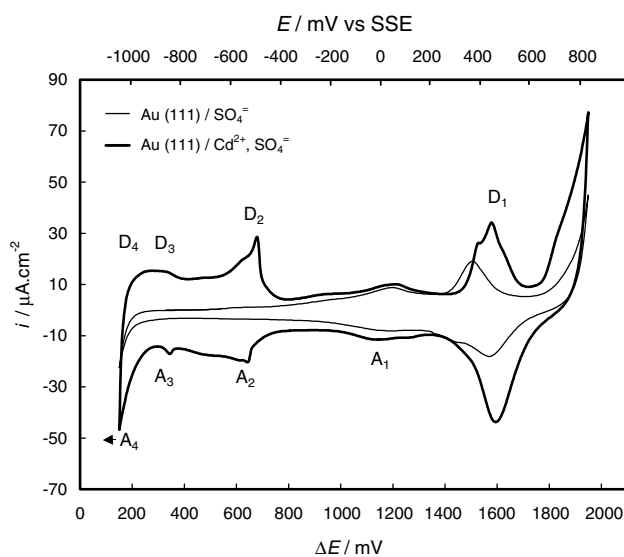


Fig. 1. Cyclic voltammograms for the systems Au(111)/5 mM H₂SO₄ + 0.1 M Na₂SO₄ (—) and Au(111)/5 mM H₂SO₄ + 0.1 M Na₂SO₄ + 1 mM CdSO₄ (---). $T = 298$ K, $|dE/dt| = 50$ mV s⁻¹.

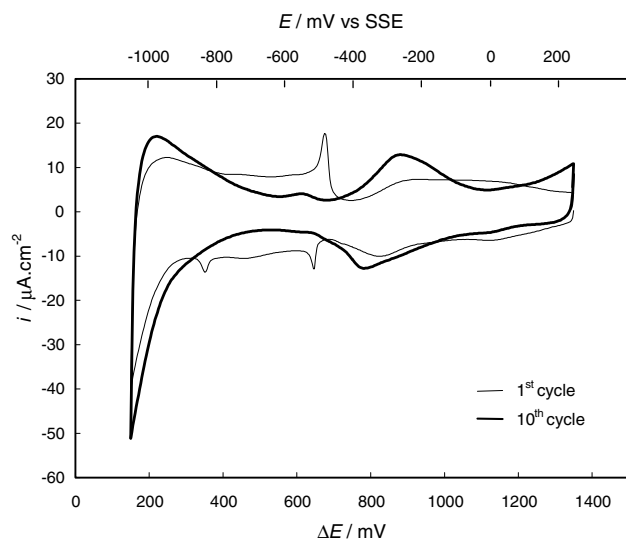


Fig. 2. Cyclic voltammogram in the system Au(111)/5 mM $\text{H}_2\text{SO}_4 + 0.1 \text{ M Na}_2\text{SO}_4 + 1 \text{ mM CdSO}_4$. $T = 298 \text{ K}$, $|dE/dt| = 50 \text{ mV s}^{-1}$. Effect of repetitive cycling in the underpotential range $150 \leq \Delta E/\text{mV} \leq 1350$.

produces a spectrum that varies with the number of cycles (Fig. 2). This result is indicative of an irreversible process, probably related to the formation of a Au–Cd alloy. In this case, the anodic limit used in the experiment would be not enough to strip the formed alloy.

In order to investigate this non-equilibrium phenomenon observed at relatively high underpotentials, long time polarization experiments were performed. The potential was stepped from $\Delta E = 1700 \text{ mV}$, i.e., an underpotential value between the peak D_1 and the oxidation of the substrate, to different lower underpotentials ΔE_k ($\Delta E_k/\text{mV} = 1350, 1150$). After maintaining the selected ΔE_k value for different polarization times, t_p , the potential was swept back recording the corresponding $\Delta E - i$ desorption spectra (Fig. 3). After the polarization at $\Delta E_k = 1350 \text{ mV}$ only the peak related to anion adsorption is present in the $\Delta E - i$ desorption spectra, and the corresponding charges do not show changes with t_p . This result is indicative that no irreversible processes related to Cd adsorption take place. On the other hand, after the polarization at $\Delta E_k = 1150 \text{ mV}$ the stripping curves also show the presence of the peak D_1 together with the peak related to the anion adsorption. The peak D_1 does not remain stable and its height increases with t_p . This observation suggests that the formation of a Au–Cd alloy phase occurs at this relatively high ΔE_k value and that the peak D_1 is related to the dissolution of this alloy. The alloy formation process can be analysed from the current–potential desorption spectra showed in Fig. 3(b). In the present case, the time-dependence of the corresponding cumulative charges, Δq vs t_p , obeys a parabolic law (Fig. 4), which is characteristic of a 3D bulk alloy [1].

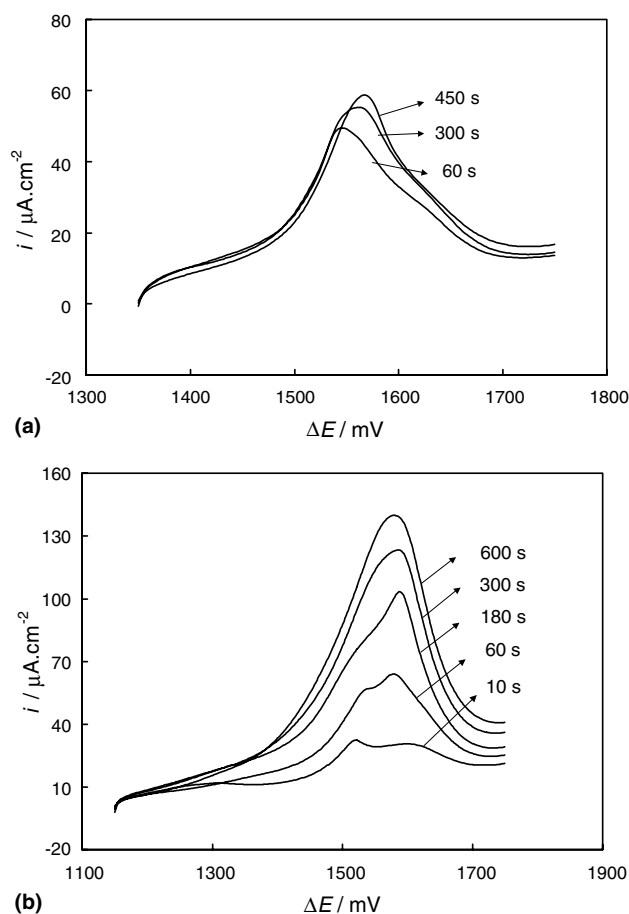


Fig. 3. Current–potential desorption spectra obtained in the system Au(111)/5 mM $\text{H}_2\text{SO}_4 + 0.1 \text{ M Na}_2\text{SO}_4 + 1 \text{ mM CdSO}_4$, after polarization during different times at (a) $\Delta E_k = 1350 \text{ mV}$, (b) $\Delta E_k = 1150 \text{ mV}$. $T = 298 \text{ K}$, $|dE/dt| = 50 \text{ mV s}^{-1}$.

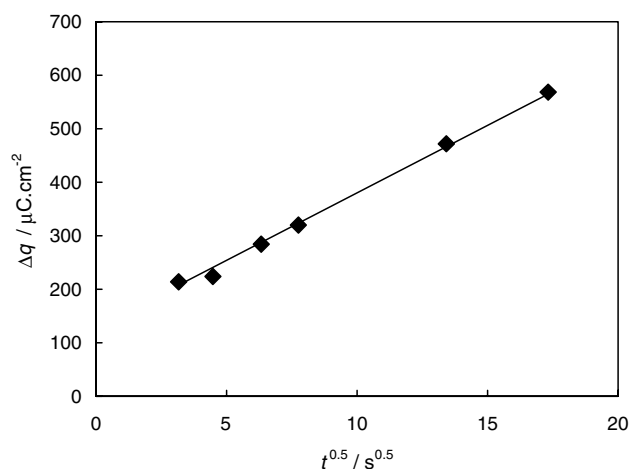


Fig. 4. Time dependence of the cumulative charge, Δq , recorded at $\Delta E_k = 1150 \text{ mV}$ in the system Au(111)/5 mM $\text{H}_2\text{SO}_4 + 0.1 \text{ M Na}_2\text{SO}_4 + 1 \text{ mM CdSO}_4$.

3.2. In situ STM studies

The changes in the surface morphology during the formation and subsequent dissolution of Cd UPD in the system Au(111)/Cd²⁺, SO₄²⁻ were followed by in situ STM analysis. In the potential range $1350 \leq \Delta E/\text{mV} \leq 1750$ it can be assumed that the Au(111) surface is nearly free of Cd. The surface consists of atomically smooth terraces separated by monatomic steps (Fig. 5(a)), in agreement with previous results obtained for Au(111) and Au(100) using the same surface preparation procedure [22,25]. At this potential range only a high surface mobility is observed which produces morphological changes of the flat terraces.

When the potential is changed to $\Delta E = 1150$ mV, a growth of steps is observed and 2D islands are formed on top of the terraces (Fig. 5(b)). These results confirm that the Cd deposition process is initiated at this relatively high underpotential. The long time polarization at this underpotential (Fig. 5(c) and (d)) promotes the growth and coalescence of the 2D islands. It is important to note that new 2D islands are generated on top of the partially formed first Cd monolayer. A representative close-up of the 2D islands is shown in Fig. 5(e). This atomically resolved image reveals an hexagonal atomic structure with interatomic spacing of 0.29 ± 0.01 nm

which corresponds, in principle, to a condensed Au(111)–(1×1)Cd structure. From the long time polarization experiments discussed previously (Figs. 3 and 4), the formation of a Au–Cd alloy was suggested at $\Delta E_k = 1150$ mV. In this case, it is difficult to know if the 2D islands formed are constituted either by Cd atoms or by Au and Cd atoms, since both atomic diameters are similar ($d_{0,\text{Au}} = 0.2884$ nm; $d_{0,\text{Cd}} = 0.2979$ nm) [26]. The nature of these 2D islands could be analyzed using in situ Distance Tunneling Spectroscopy (DTS) which makes it possible to obtain data about the nature of the substrate and adlayers [1]. The place exchange mechanism between the Au substrate atoms and the adsorbed Cd atoms could be operative, thus forming the initial stage of a highly distorted Au–Cd alloy. The further growth is assumed to take place by solid state diffusion of either Cd or Au atoms through the vacancy-rich surface alloy and simultaneous Cd deposition on modified 2D Au–Cd substrate surface [1,12,13]. Finally, when the electrode potential is shifted positively to $\Delta E = 1750$ mV the Cd layer is stripped and many holes of monatomic height are formed (Fig. 5(f)) which cause a surface roughening of the original surface. This result, also observed in other similar system [27], is another indication that the Cd atoms have reached relatively deeper zones of the electrode during the UPD process

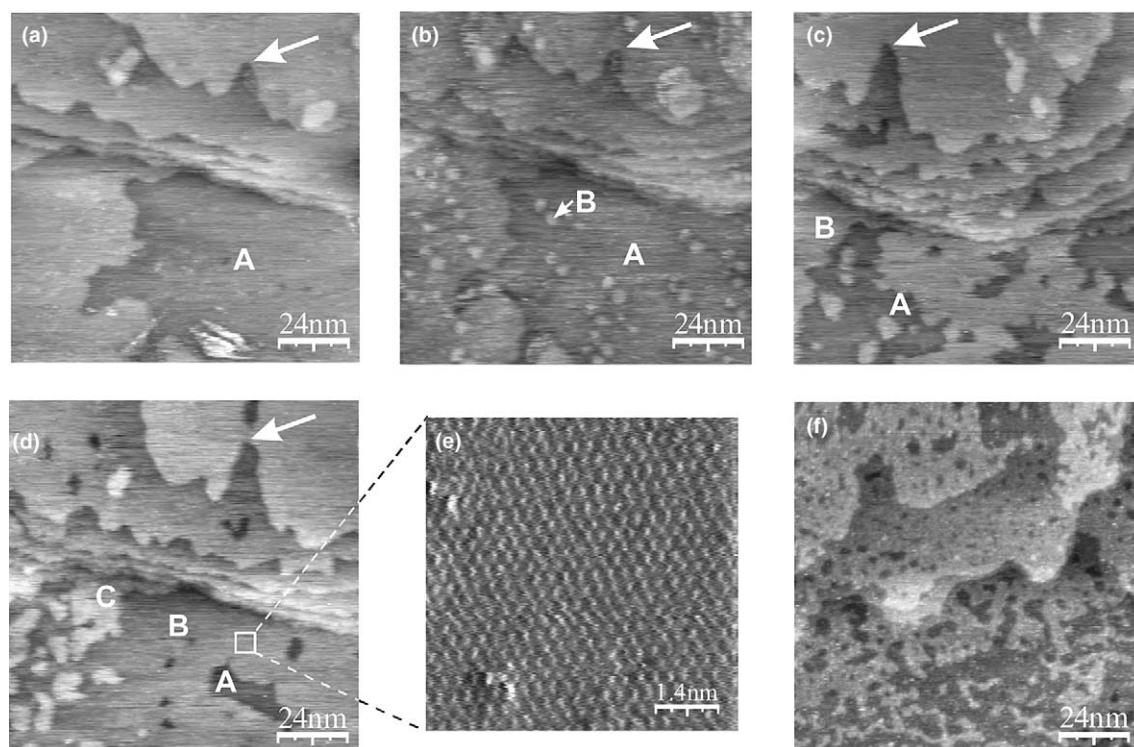


Fig. 5. In situ STM images of Cd UPD in the system Au(111)/5 mM H₂SO₄ + 0.1 M Na₂SO₄ + 1 mM CdSO₄, at $T = 298$ K and (a) $\Delta E = 1750$ mV; (b) $\Delta E = 1150$ mV, $t_p = 450$ s; (c) $\Delta E = 1150$ mV, $t_p = 800$ s; (d) $\Delta E = 1150$ mV, $t_p = 1030$ s; (e) unfiltered high resolution image of the atomic structure obtained in the area indicated in (d); (f) $\Delta E = 1750$ mV, $t_p = 900$ s. The arrows in all images indicate the location of a particular reference point of the substrate accounting for thermal drift. The letters indicate: (A) the substrate terraces; (B) first layer of Cd partially formed; (C) new 2D Cd islands formed on top of the first layer of Cd.

leading to a 3D Au–Cd bulk alloy, and that the anodic peak D_1 is really connected with the dissolution of this alloy.

As was mentioned in previous sections, the formation of a Au–Cd alloy in the system Au(1 1 1)/Cd²⁺ was also reported by other authors [15–20]. Nevertheless, in these previous works the alloying process was assumed to start in the potential range corresponding to the UPD peaks A_2/D_2 , this means at $\Delta E \approx 650$ mV. In the present work it was demonstrated that a 3D Au–Cd alloy can be formed at relatively high underpotentials ($\Delta E \approx 1150$ mV). The reason of this discrepancy, besides the difference in the UPD ranges studied, could be related to the Au(1 1 1) surface characteristics present in each case. The formation mechanism of a metal-substrate alloy strongly depends on the crystallographic orientation of the substrate and on the crystal imperfections density [1]. The other authors [6,7,15,16,18,19] have used thin films of gold on glass as substrates, with annealing in a hydrogen flame as a surface pretreatment. This procedure produces a reconstructed Au(1 1 1) surface with wide terraces. The Cd UPD occurs onto the reconstructed Au(1 1 1) without lifting the reconstruction [15,16,18,19] and this surface condition is different to the present case. In this sense, the electrochemically polished Au(1 1 1) electrode used in this work exhibit an unreconstructed surface in the total UPD range considered [25] and the surface imperfections density could be also different. In addition, the presence of sulphate anions adsorbed on the gold surface may also have an influence on the Cd adsorption and the subsequent alloy formation process. Taking into account all these observations, further work is required to analyse in more detail the mechanism of the alloy formation process observed in this system. These studies involving also DTS analysis are now in progress.

4. Conclusions

The initial stages of the Au–Cd alloy formation in the course of Cd UPD in the system Au(1 1 1)/Cd²⁺, SO₄²⁻ were examined by conventional electrochemical techniques and in situ STM. The long time polarization experiments and the current–potential desorption spectra have indicated that a 3D Au–Cd alloy can be formed at relatively high underpotentials. The Cd UPD starts with the growth of steps and the formation of 2D Cd islands as was observed by in situ STM images. These islands grow and coalesce at a constant potential with the subsequent formation of new 2D islands on top of the partially formed first Cd monolayer. Atomically resolved images of these islands have revealed an hexagonal atomic structure with an interatomic distance of

0.29 ± 0.01 nm. The dissolution of these features occurs together with the formation of many holes of monatomic height which induces a surface roughening. The alloy formation is explained considering a place exchange process between the Au atoms and the adsorbed Cd atoms followed by solid-state diffusion of these atoms through the alloyed phase.

Acknowledgements

The authors wish to thank the Universidad Nacional del Sur, Argentina, for financial support of this work. M.C. del Barrio acknowledges a fellowship granted by CONICET.

References

- [1] E. Budevski, G. Staikov, W.J. Lorenz, *Electrochemical Phase Formation and Growth*, VCH-Weinheim, 1996.
- [2] E. Herrero, L.J. Buller, H.D. Abruña, *Chem. Rev.* 101 (2001) 1897.
- [3] J.W. Schultz, F.D. Koppitz, M.M. Lohrengel, *Ber. Bunsenges. Phys. Chem.* 78 (1974) 693.
- [4] B.W. Gregory, D.W. Suggs, J.L. Stickney, *J. Electrochem. Soc.* 138 (1991) 1279.
- [5] X. Xing, D.A. Scherson, C. Mak, *J. Electrochem. Soc.* 149 (2002) C586.
- [6] S. Hsieh, A.A. Gewirth, *Langmuir* 16 (2000) 9501.
- [7] J.C. Bondos, A.A. Gewirth, R.G. Nuzzo, *J. Phys. Chem.* 100 (1996) 8617.
- [8] B.K. Niece, A.A. Gewirth, *Langmuir* 16 (2000) 6302.
- [9] G. Inzelt, G. Horányi, *J. Electroanal. Chem.* 491 (2000) 111.
- [10] R. Vidu, S. Hara, *Scr. Mater.* 41 (1999) 617.
- [11] R. Vidu, S. Hara, *J. Electroanal. Chem.* 475 (1999) 171.
- [12] R. Vidu, S. Hara, *Surf. Sci.* 452 (2000) 229.
- [13] R. Vidu, S. Hara, *Phys. Chem. Chem. Phys.* 3 (2001) 3320.
- [14] H. Kawamura, M. Takahasi, J. Mizuki, *J. Electrochem. Soc.* 149 (2002) C586.
- [15] M.D. Lay, J.L. Stickney, *J. Am. Chem. Soc.* 125 (2003) 1352.
- [16] M.D. Lay, K. Varazo, N. Srisook, J.L. Stickney, *J. Electroanal. Chem.* 554–555 (2003) 221.
- [17] D. Lee, T. Rayment, *Electrochem. Comm.* 4 (2002) 832.
- [18] S. Maupai, Y. Zhang, P. Schmuki, *Surf. Sci.* 527 (2003) L165.
- [19] S. Maupai, Y. Zhang, P. Schmuki, *Electrochem. Solid State Lett.* 6 (2003) C63.
- [20] Y. Zhang, S. Maupai, P. Schmuki, *Surf. Sci.* 551 (2004) L33.
- [21] K. Engelsmann, W.J. Lorenz, E. Schmidt, *J. Electroanal. Chem.* 114 (1980) 1.
- [22] S.G. García, D.R. Salinas, C.E. Mayer, J.R. Vilche, H.-J. Pauling, S. Vinzelberg, G. Staikov, W.J. Lorenz, *Surf. Sci.* 316 (1994) 143.
- [23] H. Angerstein-Kozłowska, B.E. Conway, A. Hamelin, L. Stoicoviciu, *J. Electroanal. Chem.* 228 (1987) 429.
- [24] P. Mrozek, M. Han, Y.-E. Sung, A. Wieckowski, *Surf. Sci.* 319 (1994) 21.
- [25] S. García, D. Salinas, C. Mayer, E. Schmidt, G. Staikov, W.J. Lorenz, *Electrochim. Acta* 43 (1998) 3007.
- [26] B.D. Cullity, *Elements of X-Ray diffraction*, second ed., Addison-Wesley, Reading, MA, 1978, p. 506.
- [27] S.G. García, D.R. Salinas, G. Staikov (in preparation).